Discrete and Continuous Dynamical Systems - Series S

doi:10.3934/dcdss.2023157

A MAGIC TWO-RELAXATION-TIME LATTICE BOLTZMANN ALGORITHM FOR MAGNETOHYDRODYNAMICS

Paul J. Dellar✉

Mathematical Institute, University of Oxford, Radcliffe Observatory Quarter
Oxford OX2 6GG, UK

Abstract. The two-relaxation-time collision operator in discrete kinetic theory models collisions between particles by grouping them into pairs with antiparallel velocities. It prescribes a linear relaxation towards equilibrium with one rate for the even combination of distribution functions for each pair, and another rate for the odd combination. We reformulate this collision operator using relaxation rates for the forward-propagating and backward-propagating combinations instead. An optimal pair of relaxation rates sets the forward-propagating combination of each pair of distributions to equilibrium. Only the backward-propagating non-equilibrium distributions remain. Applying this result twice gives closed discrete equations for evolving the macroscopic variables alone across three time levels. We split the equivalent equations into a first-order system: a conservation law and a kinetic equation for the flux. All other quantities are evaluated at equilibrium. We apply this formalism to the magnetic field in a lattice Boltzmann scheme for magnetohydrodynamics. The antisymmetric part of the kinetic equation matches the Maxwell–Faraday equation and Ohm's law. The symmetric part matches the hyperbolic divergence cleaning model. The discrete divergence of the magnetic field remains zero, to within round-off error, when the initial magnetic field is the discrete curl of a vector potential. We have thus constructed a mimetic or constrained transport scheme for magnetohydrodynamics.

1. **Introduction.** The lattice Boltzmann approach to simulating hydrodynamics represents the macroscopic variables, the fluid density and velocity, as moments of a set of distribution functions. These evolve according to a discrete velocity Boltzmann equation, such as (4) below. This is a linear, constant-coefficient hyperbolic system with algebraic terms representing a linear relaxation of the distribution functions towards some equilibrium values. The only nonlinearity in the system is through the dependence of these equilibrium values on the original macroscopic variables, as in (8) below. This simplicity comes at the price of enlarging the number of degrees of freedom. For example, the two-dimensional isothermal Navier–Stokes equations require three degrees of freedom per grid point, the fluid density and two components of velocity. The standard lattice Boltzmann scheme for these equations requires nine degrees of freedom per grid point [7, 36, 41].

Ginzburg and colleagues [16, 20, 21, 22, 24, 25, 26, 27] have extensively studied a particular form of relaxation towards equilibrium called the two-relaxation-time

2020 *Mathematics Subject Classification.* Primary: 76W05, 65M75; Secondary: 65M06.

Key words and phrases. Mimetic finite differences, constrained transport scheme, hyperbolic divergence cleaning, equivalent equations, structure-preserving discretisations.

(TRT) collision operator. This operator groups the discrete velocities into anti-parallel pairs. It prescribes one relaxation rate for the even combination of distribution functions for the two anti-parallel velocities, and another relaxation rate for the odd combination. One particular "magic" relation between these two relaxation rates places the point of zero tangential velocity precisely halfway between grid points in simulations of axis-aligned Poiseuille flow with bounce-back boundary conditions [23, 24, 27]. A different "optimal" relation between the relaxation rates enabled Ginzburg [21, 22] to derive a closed macroscopic finite difference scheme for the mass density alone from a lattice Boltzmann scheme for an advection-diffusion equation. This finite difference scheme evolves the mass density across three time levels, and reduces to the Du Fort–Frankel scheme for the diffusion equation [17]. This derivation holds much more generally than the transformations connecting specific one-dimensional, two-velocity kinetic models and the Du Fort–Frankel scheme [1, 10, 14]. Conversely, Fučík & Straka [19] and Bellotti *et al.* [3] have recently introduced algorithms to construct equivalent macroscopic finite difference schemes across multiple time levels for any lattice Boltzmann equation. The first construction needs up to $q+1$ time levels for a lattice Boltzmann equation with q discrete velocities [19]. The second construction needs up to $q+1-n$ time levels for a lattice Boltzmann equation with q discrete velocities and n conserved moments [3]. Bellotti *et al.* [3] have used a special case of their algorithm to construct finite difference schemes across three time levels from lattice Boltzmann equations with optimal TRT collision operators.

In this work we re-interpret the TRT collision operator as prescribing different relaxation rates for the forward-propagating and backward-propagating parts of each pair of distribution functions with anti-parallel velocities. The optimal combination of relaxation rates then sets the forward-propagating part to equilibrium. By considering two successive timesteps of this lattice Boltzmann equation, we can derive a closed macroscopic finite difference scheme across three time levels for any moment of the distributions, generalising Ginzburg's results [21, 22]. Moreover, we argue that the macroscopic finite difference scheme is best interpreted as a discretisation of a first order system. One half of this system is a conservation law of the expected kind, and the other is a separate evolution equation for the flux in the conservation law. The latter contains no further kinetic degrees of freedom.

We apply this interpretation to a lattice Boltzmann formulation for evolving the magnetic field in resistive magnetohydrodynamics (MHD). The MHD equations provide a fluid description of materials containing two or more species of different charges, such as electrolytes, liquid metals, and plasmas [8]. The magnetic field evolves according to Maxwell's equations, which in particular require the divergence of the magnetic field to vanish. This property is often not satisfied in numerical simulations, or only satisfied to within the spatial truncation error, which can cause artifacts in solutions [5, 52]. We will show that our closed macroscopic finite difference scheme for the magnetic field implies another closed finite difference scheme for evolving a particular finite difference approximation of the divergence of the magnetic field. This discrete divergence obeys a discrete analog of the telegraph equation, so our formulation implements an extended set of Maxwell's equations that support hyperbolic divergence cleaning [2, 9, 15, 43]. Moreover, the discrete divergence remains zero, to within floating point round-off error, if it is zero initially. Our scheme thus qualifies as a mimetic finite difference scheme [33, 37, 43], or equivalently as a constrained transport scheme for the magnetic field [18, 52].

2. **Kinetic formulation for magnetohydrodynamics.** The magnetic field in an electrically conducting fluid evolves according to a combination of the Maxwell–Faraday equation and Ohm's law [8]

$$\partial_t \mathbf{B} + \nabla\times\mathbf{E} = 0, \quad \mathbf{E} + \mathbf{u}\times\mathbf{B} = \eta\mathbf{J}, \tag{1}$$

where $\mathbf{E}$ and $\mathbf{B}$ are the electric and magnetic fields, $\mathbf{u}$ the fluid velocity, and η the resistivity (assumed to be constant). Evolution under these equations preserves $\nabla\cdot\mathbf{B} = 0$, provided it holds initially, because $\nabla\cdot(\nabla\times\mathbf{E}) \equiv 0$ for all vector fields $\mathbf{E}$.

The equations for compressible resistive magnetohydrodynamics with an isothermal equation of state are thus

$$\partial_t \rho + \nabla\cdot(\rho\mathbf{u}) = 0, \tag{2a}$$

$$\partial_t(\rho\mathbf{u}) + \nabla\cdot(\rho\mathbf{u}\mathbf{u} + \rho\theta\mathsf{I}) = \mathbf{J}\times\mathbf{B} + \nabla\cdot(\mu\mathbf{S}), \tag{2b}$$

$$\partial_t \mathbf{B} = \nabla\times(\mathbf{u}\times\mathbf{B} - \eta\mathbf{J}), \tag{2c}$$

where ρ is the fluid density, $\mathbf{J}$ the electric current, $\mathbf{S} = (\nabla\mathbf{u}) + (\nabla\mathbf{u})^{\mathsf{T}}$ the symmetric strain rate tensor, I the identity tensor, θ the temperature in energy units, and μ the dynamic viscosity. The electric current is $\mathbf{J} = \nabla\times\mathbf{B}$, in suitable electromagnetic units, under the non-relativistic approximation that holds when the fluid velocity $|\mathbf{u}|$ is much smaller than the speed of light c. See Sec. 7.1 for details. The magnetic field exerts a Lorentz force $\mathbf{J}\times\mathbf{B}$ on the fluid, and is in turn advected by, and diffuses through, the fluid according to the induction equation (2c).

2.1. **Hydrodynamics.** We represent the density and momentum equations using a standard hydrodynamic lattice Boltzmann formulation [7, 36, 41]. The fluid density, momentum and momentum flux $\mathbf{\Pi}$ are given by moments of a set of N scalar distribution functions f_k with associated discrete velocities $\boldsymbol{\xi}_k$ for $k = 0, \ldots, N-1$,

$$\rho = \sum_{k=0}^{N-1} f_k, \quad \rho\mathbf{u} = \sum_{k=0}^{N-1} \boldsymbol{\xi}_k f_k, \quad \mathbf{\Pi} = \sum_{k=0}^{N-1} \boldsymbol{\xi}_k\boldsymbol{\xi}_k f_k. \tag{3}$$

The f_k are postulated to evolve according to the discrete velocity Boltzmann equation

$$\partial_t f_k + \boldsymbol{\xi}_k\cdot\nabla f_k = -\frac{1}{\tau}\left(f_k - f_k^{(0)}\right). \tag{4}$$

The single-relaxation-time collision operator on the right-hand side relaxes the f_k towards some equilibria $f_k^{(0)}$ that are prescribed functions of the macroscopic variables ρ, $\mathbf{u}$ and $\mathbf{B}$. Taking moments of (4) gives the mass conservation equation (2a) and a momentum conservation equation in the form

$$\partial_t(\rho\mathbf{u}) + \nabla\cdot\mathbf{\Pi} = 0. \tag{5}$$

The right-hand sides of (2a) and (5) vanish because the construction of the $f_k^{(0)}$ from the f_k ensures that the collision operator on the right-hand side of (4) conserves mass and momentum,

$$\sum_{k=0}^{N-1} f_k^{(0)} = \sum_{k=0}^{N-1} f_k, \quad \sum_{k=0}^{N-1} \boldsymbol{\xi}_k f_k^{(0)} = \sum_{k=0}^{N-1} \boldsymbol{\xi}_k f_k. \tag{6}$$

The momentum equation (2b) can be rewritten in the conservation form (5) with $\mathbf{\Pi} = \mathbf{\Pi}^{(0)} - \mu\mathbf{S}$ for the equilibrium momentum flux

$$\mathbf{\Pi}^{(0)} = \rho\mathbf{u}\mathbf{u} + \rho\theta\mathsf{I} + \tfrac{1}{2}|\mathbf{B}|^2\,\mathsf{I} - \mathbf{B}\mathbf{B}. \tag{7}$$

We have used $\nabla\cdot\mathbf{B} = 0$ to write the Lorentz force $\mathbf{J}\times\mathbf{B} = (\nabla\times\mathbf{B})\times\mathbf{B}$ as the divergence of a Maxwell stress with an isotropic magnetic pressure $\frac{1}{2}|\mathbf{B}|^2$ and a magnetic tension $\mathbf{BB}$ along field lines. The equilibrium distributions are thus [11, 41]

$$f_k^{(0)} = w_k \left(\rho + \frac{1}{\theta}\rho\mathbf{u}\cdot\boldsymbol{\xi}_k + \frac{1}{2\theta^2}\boldsymbol{\xi}_k\cdot\widehat{\boldsymbol{\Pi}}^{(0)}\cdot\boldsymbol{\xi}_k - \frac{1}{2\theta}\operatorname{Tr}\widehat{\boldsymbol{\Pi}}^{(0)} \right), \tag{8}$$

where $\widehat{\boldsymbol{\Pi}}^{(0)} = \boldsymbol{\Pi}^{(0)} - \rho\theta\mathsf{I}$ is the equilibrium momentum flux minus the fluid pressure, and the w_k are quadrature weights associated with the velocities $\boldsymbol{\xi}_k$. The temperature θ is a constant defined by the isotropy condition

$$\sum_{k=0}^{N-1} w_k \boldsymbol{\xi}_k \boldsymbol{\xi}_k = \theta\mathsf{I}. \tag{9}$$

Seeking slowly varying solutions of (4) via a Chapman–Enskog expansion is equivalent to expanding $\boldsymbol{\Pi} = \boldsymbol{\Pi}^{(0)} + \boldsymbol{\Pi}^{(1)} + \cdots$ while leaving ρ, $\mathbf{u}$ and $\mathbf{B}$ unexpanded. The leading order term $\boldsymbol{\Pi}^{(0)}$ gives the momentum equation for ideal magnetohydrodynamics. The first correction $\boldsymbol{\Pi}^{(1)} = -\mu\mathbf{S}$ is a Newtonian viscous stress with dynamic viscosity $\mu = \tau\rho\theta$, to within an error that can be neglected when the fluid velocity $\mathbf{u}$ and Alfvén velocity $\mathbf{B}\rho^{-1/2}$ are both much smaller than the sound speed $\theta^{1/2}$ [11, 32, 42].

2.2. **Magnetic field.** We can rewrite the Faraday–Maxwell equation (1) for evolving $\mathbf{B}$ as

$$\partial_t\mathbf{B} + \nabla\cdot\boldsymbol{\Lambda} = 0, \tag{10}$$

where $\boldsymbol{\Lambda}$ is a rank-2 tensor. The two are exactly equivalent if $\Lambda_{\alpha\beta} = -\epsilon_{\alpha\beta\gamma}E_\gamma$ is antisymmetric, but we will need to accommodate the symmetric part of $\boldsymbol{\Lambda}$ in our kinetic formulation. Equation (10) resembles the momentum equation (5), but the momentum flux tensor $\boldsymbol{\Pi}$ defined in (3) is symmetric by construction, while $\boldsymbol{\Lambda}$ is not. We therefore cannot represent $\mathbf{B}$ using scalar distribution functions [11].

Instead, we introduce a set of M vector-valued distribution functions $\mathbf{g}_k$ such that

$$\mathbf{B} = \sum_{k=0}^{M-1} \mathbf{g}_k, \quad \boldsymbol{\Lambda} = \sum_{k=0}^{M-1} \boldsymbol{\xi}_k\mathbf{g}_k. \tag{11}$$

These functions are postulated to evolve according to [11]

$$\partial_t\mathbf{g}_k + \boldsymbol{\xi}_k\cdot\nabla\mathbf{g}_k = -\frac{1}{\tau_M}\left(\mathbf{g}_k - \mathbf{g}_k^{(0)}\right), \tag{12}$$

where again we use a collision operator with a single relaxation time τ_M on the right-hand side for simplicity. The equilibrium distributions are [11]

$$\mathbf{g}_k^{(0)} = W_k\left(\mathbf{B} + \Theta^{-1}\boldsymbol{\xi}_k\cdot\boldsymbol{\Lambda}^{(0)}\right), \text{ with } \boldsymbol{\Lambda}^{(0)} = \mathbf{u}\,\mathbf{B} - \mathbf{B}\,\mathbf{u}. \tag{13}$$

Taking the zeroth moment of (12) thus gives (10), because the $\mathbf{g}_k^{(0)}$ are constructed so that collisions conserve the magnetic field $\mathbf{B}$. The first moment of (12) gives

$$\partial_t\boldsymbol{\Lambda} + \nabla\cdot\mathbf{M} = -\frac{1}{\tau_M}\left(\boldsymbol{\Lambda} - \boldsymbol{\Lambda}^{(0)}\right), \text{ where } \mathbf{M} = \sum_{k=0}^{M-1}\boldsymbol{\xi}_k\boldsymbol{\xi}_k\mathbf{g}_k. \tag{14}$$

The number of discrete velocities M, weights W_k, and lattice constant Θ defined by the isotropy condition

$$\sum_{k=0}^{M-1} W_k \boldsymbol{\xi}_k \boldsymbol{\xi}_k = \Theta \mathsf{I}, \tag{15}$$

can all be different from those used in the hydrodynamic formulation above. In principle, the set of discrete velocities can be completely different too.

Seeking slowly varying solutions of (12) via a Chapman–Enskog expansion is equivalent to expanding $\boldsymbol{\Lambda} = \boldsymbol{\Lambda}^{(0)} + \boldsymbol{\Lambda}^{(1)} + \cdots$ and $\mathbf{M} = \mathbf{M} + \mathbf{M}^{(1)} + \cdots$ while leaving ρ, $\mathbf{u}$ and $\mathbf{B}$ unexpanded. The leading order term from (13) gives the ideal MHD induction equation, while the first correction $\boldsymbol{\Lambda}^{(1)} = -\tau_M \Theta \nabla \mathbf{B}$ gives the resistive MHD induction equation with constant resistivity $\eta = \tau_M \Theta$ in the form

$$\partial_t \mathbf{B} + \nabla \cdot (\mathbf{u}\,\mathbf{B} - \mathbf{B}\,\mathbf{u}) = \eta \nabla^2 \mathbf{B}. \tag{16}$$

This equation can be rewritten as

$$\partial_t \mathbf{B} = \nabla \times (\mathbf{u} \times \mathbf{B} - \eta \nabla \times \mathbf{B}) + \eta \nabla (\nabla \cdot \mathbf{B}), \tag{17}$$

where the first term on the right-hand side matches (2c) above. The two equations exactly coincide if $\nabla \cdot \mathbf{B} = 0$, but (17) also includes a parabolic divergence cleaning term [9, 15]. Taking the divergence of (17) gives a diffusion equation for $\nabla \cdot \mathbf{B}$,

$$\partial_t (\nabla \cdot \mathbf{B}) = \eta \nabla^2 (\nabla \cdot \mathbf{B}), \tag{18}$$

in contrast to the Faraday–Maxwell equation that implies $\partial_t (\nabla \cdot \mathbf{B}) = 0$. This is discussed in Sec. 7.2.

2.3. **Coupling.** The hydrodynamic and magnetic parts are coupled only through the macroscopic variables $\mathbf{u}$ and $\mathbf{B}$ that appear in both sets of equilibrium distributions. This is a modular formulation that easily acccommodates changes to either part. By contrast, an earlier lattice Boltzmann formulation for magnetohydrodynamics used one set of tensorial distribution functions f_{jk} to represent both $\mathbf{u}$ and $\mathbf{B}$ [40]. We can use different sets of discrete velocities for the hydrodynamic and magnetic parts. A popular choice in two dimensions use the D2Q9 lattice for the f_k and two copies of the D2Q5 lattice for the two components of the vectors $\mathbf{g}_k$, as illustrated in Fig. 1. The corresponding weights are [11, 41]

$$w_0 = 4/9, \quad w_{1,2,3,4} = 1/9, \quad w_{6,7,8,9} = 1/36, \quad W_0 = 1/3, \quad W_{1,2,3,4} = 1/6. \tag{19}$$

The lattice constants defined by (9) and (15) are then equal, $\theta = \Theta = 1/3$.

3. **Two-relaxation-time magnetic collision operator.** We now consider a generalisation of the single-relaxation-time collision operator in the kinetic equation (12) for the $\mathbf{g}_k$. The two-relaxation-time or TRT collision operator groups the discrete velocities into anti-parallel pairs $\boldsymbol{\xi}_k$ and $\boldsymbol{\xi}_{\overline{k}} = -\boldsymbol{\xi}_k$ [16, 20, 21, 22, 24, 25, 26, 27]. This relation defines $\overline{k}$ as a function of k. The anti-parallel pairs are called "links", or "dumbbells" in the context of lattice gas collision operators [46]. The TRT collision operator applies different relaxation times τ_o and τ_e to the odd and even parts of the distribution functions, as defined by the decomposition

$$\mathbf{g}_k = \frac{1}{2}\left(\mathbf{g}_k + \mathbf{g}_{\overline{k}}\right) + \frac{1}{2}\left(\mathbf{g}_k - \mathbf{g}_{\overline{k}}\right) = \left(\mathbf{g}_k\right)_{\mathsf{even}} + \left(\mathbf{g}_k\right)_{\mathsf{odd}}. \tag{20}$$

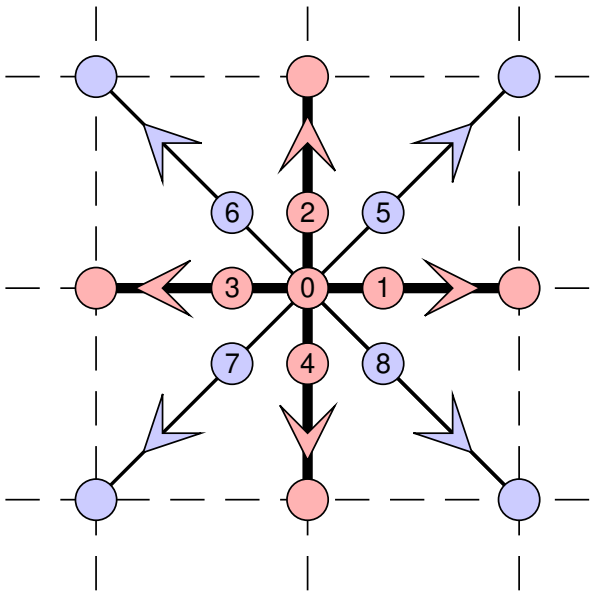

FIGURE 1. The nine velocities $\boldsymbol{\xi}_0, \ldots, \boldsymbol{\xi}_8$ form the D2Q9 lattice used for the f_k. The five velocities $\boldsymbol{\xi}_0, \ldots, \boldsymbol{\xi}_4$ (thicker lines) form the D2Q5 lattice used for the components of the $\mathbf{g}_k$.

This is equivalent to applying the odd relaxation time τ_o to the odd moment $\boldsymbol{\Lambda}$, and the even relaxation time τ_e to the even moment $\mathbf{M}$. The evolution equation for the $\mathbf{g}_k$ thus becomes

$$\partial_t \mathbf{g}_k + \boldsymbol{\xi}_k \cdot \nabla \mathbf{g}_k = -\frac{1}{\tau_\mathsf{e}} \left(\mathbf{g}_k - \mathbf{g}_k^{(0)} \right)_\mathsf{even} - \frac{1}{\tau_\mathsf{o}} \left(\mathbf{g}_k - \mathbf{g}_k^{(0)} \right)_\mathsf{odd}. \tag{21}$$

Discretising (21) in space and time using either Strang splitting [13, 49] or an integration along characteristics using the trapezium rule followed by a change of variables [12, 30] leads to the discrete evolution equation

$$\begin{aligned} \widetilde{\mathbf{g}}_k(\mathbf{x} + \boldsymbol{\xi}_k \Delta t, t + \Delta t) = \widetilde{\mathbf{g}}_k(\mathbf{x}, t) &- \omega_\mathsf{e} \left(\widetilde{\mathbf{g}}_k(\mathbf{x}, t) - \mathbf{g}_k^{(0)}(\mathbf{x}, t) \right)_\mathsf{even} \\ &- \omega_\mathsf{o} \left(\widetilde{\mathbf{g}}_k(\mathbf{x}, t) - \mathbf{g}_k^{(0)}(\mathbf{x}, t) \right)_\mathsf{odd}, \end{aligned} \tag{22}$$

for the transformed variables

$$\widetilde{\mathbf{g}}_k = \mathbf{g}_k + \frac{\Delta t}{2\tau_\mathsf{e}} \left(\mathbf{g}_k - \mathbf{g}_k^{(0)} \right)_\mathsf{even} + \frac{\Delta t}{2\tau_\mathsf{o}} \left(\mathbf{g}_k - \mathbf{g}_k^{(0)} \right)_\mathsf{odd}. \tag{23}$$

The even and odd discrete relaxation rates include the Hénon [31] correction of the relaxation times from $\tau_{\mathsf{e},\mathsf{o}}$ to $\tau_{\mathsf{e},\mathsf{o}} + \Delta t/2$ that arises from discretising (21),

$$\omega_\mathsf{e} = \frac{\Delta t}{\tau_\mathsf{e} + \Delta t/2}, \quad \omega_\mathsf{o} = \frac{\Delta t}{\tau_\mathsf{o} + \Delta t/2}. \tag{24}$$

The discrete evolution under (22) of the transformed variables approximates the continuous evolution under (21) with second-order accuracy in Δt. The transformation (23) is equivalent to the application of collisions for half a timestep to create a symmetric Strang splitting between advection and collisions [13, 49]. We can rewrite (22) more simply as

$$\begin{aligned} \widetilde{\mathbf{g}}_k(\mathbf{x} + \boldsymbol{\xi}_k \Delta t, t + \Delta t) = \widetilde{\mathbf{g}}_k(\mathbf{x}, t) &- \omega_\mathsf{f} \left(\widetilde{\mathbf{g}}_k(\mathbf{x}, t) - \mathbf{g}_k^{(0)}(\mathbf{x}, t) \right) \\ &- \omega_\mathsf{b} \left(\widetilde{\mathbf{g}}_{\overline{k}}(\mathbf{x}, t) - \mathbf{g}_{\overline{k}}^{(0)}(\mathbf{x}, t) \right), \end{aligned} \tag{25}$$

by defining the forward and backward relaxation rates

$$\omega_{\mathsf{f}} = \frac{1}{2}(\omega_{\mathsf{e}} + \omega_{\mathsf{o}}), \quad \omega_{\mathsf{b}} = \frac{1}{2}(\omega_{\mathsf{e}} - \omega_{\mathsf{o}}). \tag{26}$$

The combination of odd and even relaxation times with $\tau_{\mathsf{e}}\tau_{\mathsf{o}} = (1/4)\Delta t^2$ was named the "optimal two-relaxation-time" or OTRT model by Ginzburg and colleagues [16, 21, 25, 26]. This combination of relaxation times reduces the recurrence relation satisfied by the distribution functions in a steady solution of the general TRT lattice Boltzmann equation to an explicit formula for the distribution functions at each lattice point in terms of the equilibrium distributions at the same lattice point and its neighbours [16]. It also reduces the characteristic polynomials governing the stability of plane wave solutions of lattice Boltzmann equations for advection-diffusion equations to quadratic polynomials [26]. An optimal TRT lattice Boltzmann equation for an advection-diffusion equation can be reduced to a macroscopic finite difference scheme for the density across three time levels [21, 22].

The optimal TRT combination $\tau_{\mathsf{e}}\tau_{\mathsf{o}} = (1/4)\Delta t^2$ sets the forward relaxation rate to unity in our notation,

$$\omega_{\mathsf{f}} = \frac{1}{2}\left(\frac{\Delta t}{\Delta t^2/(4\tau_{\mathsf{o}}) + \Delta t/2} + \frac{\Delta t}{\tau_{\mathsf{o}} + \Delta t/2}\right) = 1, \tag{27}$$

so the forward-propagating part of the distribution is set to equilibrium during the collision step,

$$\widetilde{\mathbf{g}}_k(\mathbf{x} + \boldsymbol{\xi}_k\Delta t, t + \Delta t) = \mathbf{g}_k^{(0)}(\mathbf{x}, t) - \omega_{\mathsf{b}}\left(\widetilde{\mathbf{g}}_{\overline{k}}(\mathbf{x}, t) - \mathbf{g}_{\overline{k}}^{(0)}(\mathbf{x}, t)\right). \tag{28}$$

The right-hand side only involves the backward-propagating distributions $\widetilde{\mathbf{g}}_{\overline{k}}$ and the forward- and backward-propagating equilibria $\mathbf{g}_k^{(0)}$ and $\mathbf{g}_{\overline{k}}^{(0)}$. It does not involve the forward-propagating distributions $\widetilde{\mathbf{g}}_k$.

Applying (28) for two timesteps gives

$$\begin{aligned}\widetilde{\mathbf{g}}_k(\mathbf{x}, t + \Delta t) = \mathbf{g}_k^{(0)}(\mathbf{x} - \boldsymbol{\xi}_k\Delta t, t) + \omega_{\mathsf{b}}\left(\mathbf{g}_{\overline{k}}^{(0)}(\mathbf{x} - \boldsymbol{\xi}_k\Delta t, t) - \mathbf{g}_{\overline{k}}^{(0)}(\mathbf{x}, t - \Delta t)\right) \\ + \omega_{\mathsf{b}}^2\left(\widetilde{\mathbf{g}}_k(\mathbf{x}, t - \Delta t) - \mathbf{g}_k^{(0)}(\mathbf{x}, t - \Delta t)\right).\end{aligned} \tag{29}$$

The right-hand side now depends on the distributions $\widetilde{\mathbf{g}}_k$ at the same point $\mathbf{x}$ at the earlier time $t - \Delta t$. The only coupling to the adjacent points $\mathbf{x} - \boldsymbol{\xi}_k\Delta t$ is though the equilibria $\mathbf{g}_k^{(0)}$ and $\mathbf{g}_{\overline{k}}^{(0)}$.

Taking any moment $\mathcal{M}$ of (29) thus gives an expression for $\mathcal{M}(\mathbf{x}, t + \Delta t)$ in terms of $\mathcal{M}(\mathbf{x}, t - \Delta t)$, the equilibrium moment $\mathcal{M}^{(0)}(\mathbf{x}, t - \Delta t)$, and moments of the equilibrium distributions $\mathbf{g}_k^{(0)}$ and $\mathbf{g}_{\overline{k}}^{(0)}$ at adjacent points. The latter are known functions of $\mathbf{u}$ and $\mathbf{B}$ via (13). This generalises an earlier result by Ginzburg [21, 22] for the scalar diffusion equation, and provides a simpler derivation based on the optimal combination of τ_{e} and τ_{o} being equivalent to setting the forward relaxation rate $\omega_{\mathsf{f}} = 1$, so $\widetilde{\mathbf{g}}_k(\mathbf{x}, t)$ does not appear on the right-hand side of (28).

4. **Discrete evolution equation for the magnetic field.** Taking the zeroth moment of (29) gives a closed evolution equation for $\mathbf{B}$ across three time levels. The last term proportional to ω_{b}^2 vanishes, because $\mathbf{B}$ is conserved under collisions,

so

$$\mathbf{B}(\mathbf{x},t+\Delta t) = -\omega_\mathsf{b}\mathbf{B}(\mathbf{x},t-\Delta t) + \sum_{k=0}^{M-1} \mathbf{g}_k^{(0)}(\mathbf{x}-\boldsymbol{\xi}_k\Delta t,t) + \omega_\mathsf{b}\sum_{k=0}^{M-1} \mathbf{g}_k^{(0)}(\mathbf{x}+\boldsymbol{\xi}_k\Delta t,t). \tag{30}$$

The last term has been converted to a sum over k using $\boldsymbol{\xi}_k = -\boldsymbol{\xi}_{\overline{k}}$. We can evaluate the sums using

$$\sum_{k=0}^{M-1} \mathbf{g}_k^{(0)}(\mathbf{x}\pm\boldsymbol{\xi}_k\Delta t,t) = \sum_{k=0}^{M-1} W_k\mathbf{B}(\mathbf{x}+\boldsymbol{\xi}_k\Delta t,t) \pm \frac{1}{\Theta}\sum_{k=0}^{M-1} W_k\boldsymbol{\xi}_k\cdot\boldsymbol{\Lambda}^{(0)}(\mathbf{x}+\boldsymbol{\xi}_k\Delta t,t) \tag{31}$$

to obtain

$$\begin{aligned}\mathbf{B}(\mathbf{x},t+\Delta t) = &-\omega_\mathsf{b}\mathbf{B}(\mathbf{x},t-\Delta t) + (1+\omega_\mathsf{b})\sum_{k=0}^{M-1} W_k\mathbf{B}(\mathbf{x}+\boldsymbol{\xi}_k\Delta t,t) \\ &- (1-\omega_\mathsf{b})\,\frac{1}{\Theta}\sum_{k=0}^{M-1} W_k\boldsymbol{\xi}_k\cdot\boldsymbol{\Lambda}^{(0)}(\mathbf{x}+\boldsymbol{\xi}_k\Delta t,t).\end{aligned} \tag{32}$$

This is an evolution equation for $\mathbf{B}$ across the three time levels $t+\Delta t$, t and $t-\Delta t$ that also involves the velocity field $\mathbf{u}$ at the intermediate time level t via $\boldsymbol{\Lambda}^{(0)}$.

Substituting $\omega_\mathsf{b} = (\tau_\mathsf{o}-\Delta t/2)/(\tau_\mathsf{o}+\Delta t/2)$ and multiplying by $\tau_\mathsf{o}+\Delta t/2$ gives the more time-symmetric form

$$\begin{aligned}&\tau_\mathsf{o}\frac{\mathbf{B}(\mathbf{x},t+\Delta t)-2\mathbf{B}(\mathbf{x},t)+\mathbf{B}(\mathbf{x},t-\Delta t)}{\Delta t^2} + \frac{\mathbf{B}(\mathbf{x},t+\Delta t)-\mathbf{B}(\mathbf{x},t-\Delta t)}{2\Delta t} \\ &= \frac{2\tau_\mathsf{o}}{\Delta t^2}\left(\sum_{k=0}^{M-1} W_k\mathbf{B}(\mathbf{x}+\boldsymbol{\xi}_k\Delta t,t) - \mathbf{B}(\mathbf{x},t)\right) - \frac{1}{\Theta\Delta t}\sum_{k=0}^{M-1} W_k\boldsymbol{\xi}_k\cdot\boldsymbol{\Lambda}^{(0)}(\mathbf{x}+\boldsymbol{\xi}_k\Delta t,t),\end{aligned} \tag{33}$$

where $\mathbf{B}(\mathbf{x},t)$ is outside the sum. The left-hand side now contains centred finite difference approximations to the first and second derivatives with respect to time. The right-hand side contains finite difference approximations adapted to the lattice for $\nabla^2\mathbf{B}$ and $\nabla\cdot\boldsymbol{\Lambda}^{(0)}$ at the intermediate time level t (see appendix). Expanding (33) for small Δt with τ_o fixed thus gives the telegraph equation

$$\tau_\mathsf{o}\partial_{tt}\mathbf{B} + \partial_t\mathbf{B} = \tau_\mathsf{o}\Theta\nabla^2\mathbf{B} - \nabla\cdot\boldsymbol{\Lambda}^{(0)} + \mathcal{O}(\Delta t^2). \tag{34}$$

This equation supports plane-wave solutions with $\mathbf{B}(\mathbf{x},t) = B_0\mathbf{e}_y\exp(i(kx-\omega t))$, where B_0 is a constant and $\mathbf{e}_y$ is a unit vector in the y direction. These solutions describe axis-aligned electromagnetic waves propagating in a fluid at rest with $\mathbf{u}=0$ and hence $\boldsymbol{\Lambda}^{(0)}=0$. Their frequency ω is given by the dispersion relation

$$\omega^2 + \frac{i\omega}{\tau_\mathsf{o}} = \Theta k^2. \tag{35}$$

These waves propagate with phase speed $\Theta^{1/2}$ when τ_o is large enough for attenuation to be negligible, The discrete equation (33) has solutions of the same form when ω satisfies the discrete dispersion relation

$$\sin^2\left(\frac{\omega\Delta t}{2}\right) + i\frac{\Delta t}{4\tau_\mathsf{o}}\sin(\omega\Delta t) = \Theta\sin^2\left(\frac{k\Delta t}{2}\right). \tag{36}$$

This reduces to the previous dispersion relation with second-order accuracy when the frequency ω and wavenumber k are small enough for discrete effects to be negligible.

Following Ginzburg [21, 22] we can interpret (33) as a Du Fort–Frankel [17] discretisation of a diffusion equation for $\mathbf{B}$ with an additional source term from $\nabla\cdot\mathbf{\Lambda}^{(0)}$ at the intermediate time level t. Du Fort & Frankel [17] introduced their discretisation as a stabilised variant of the explicit leapfrog time discretisation scheme for the diffusion equation, but it can also be interpreted as a discretisation of a telegraph equation [17, 28, 50]. However, it will be more illuminating to treat (33) as the discretisation of a first order system instead, as described in Sec. 7.

5. **Discrete evolution equation for the discrete divergence.** The discrete evolution equation (33) for the magnetic field contains a discrete divergence operator acting on $\mathbf{\Lambda}^{(0)}$. We can define a natural discrete divergence Δ of the magnetic field by applying the same operator to $\mathbf{B}$,

$$\Delta(\mathbf{x},t) = \frac{1}{\Theta\Delta t}\sum_{j=0}^{M-1} W_j\boldsymbol{\xi}_j\cdot\mathbf{B}(\mathbf{x}+\boldsymbol{\xi}_j\Delta t,t). \tag{37}$$

The contribution from rest particles with $j=0$ vanishes because $\boldsymbol{\xi}_0=0$. This definition of Δ corresponds to the standard centred finite difference approximation to $\nabla\cdot\mathbf{B}$ on the D2Q5 and D3Q7 lattices, as $W_j=\Theta/2$ for $j\neq 0$. For the D2Q5 lattice, we obtain

$$\begin{aligned}\Delta(\mathbf{x},t) = \frac{1}{2\Delta t}\big(&B_x(\mathbf{x}+\mathbf{e}_x\Delta t,t) - B_x(\mathbf{x}-\mathbf{e}_x\Delta t,t)\\ &+B_y(\mathbf{x}+\mathbf{e}_y\Delta t,t) - B_y(\mathbf{x}-\mathbf{e}_y\Delta t,t)\big),\end{aligned} \tag{38}$$

where $\mathbf{e}_x$ and $\mathbf{e}_y$ are unit vectors in the x and y directions.

Applying the discrete divergence operator to (33) gives a closed discrete telegraph equation for Δ,

$$\begin{aligned}&\tau_\mathrm{o}\frac{\Delta(\mathbf{x},t+\Delta t)-2\Delta(\mathbf{x},t)+\Delta(\mathbf{x},t-\Delta t)}{\Delta t^2} + \frac{\Delta(\mathbf{x},t+\Delta t)-\Delta(\mathbf{x},t-\Delta t)}{2\Delta t}\\ &= \frac{2\tau_\mathrm{o}}{\Delta t^2}\left(\sum_{k=0}^{M-1} W_k\Delta(\mathbf{x}+\boldsymbol{\xi}_k\Delta t,t) - \Delta(\mathbf{x},t)\right),\end{aligned} \tag{39}$$

where $\Delta(\mathbf{x},t)$ is outside the sum. The contribution from $\mathbf{\Lambda}^{(0)}$ vanishes,

$$\sum_{j=0}^{M-1}\sum_{k=0}^{M-1} W_jW_k\xi_{j\alpha}\xi_{k\beta}\Lambda^{(0)}_{\alpha\beta}(\mathbf{x}+\boldsymbol{\xi}_k\Delta t+\boldsymbol{\xi}_j\Delta t,t) = 0, \tag{40}$$

because $\mathbf{\Lambda}^{(0)}$ is an antisymmetric tensor. Expanding (39) for small Δt gives the telegraph equation

$$\tau_\mathrm{o}\partial_{tt}(\nabla\cdot\mathbf{B}) + \partial_t(\nabla\cdot\mathbf{B}) = \tau_\mathrm{o}\Theta\nabla^2(\nabla\cdot\mathbf{B}) + \mathcal{O}(\Delta t^2). \tag{41}$$

This coincides with the evolution equation for $\nabla\cdot\mathbf{B}$ derived from an extended set of Maxwell equations that includes hyperbolic divergence cleaning (see Sec. 7.2).

We now expect $\Delta=0$ to be preserved exactly by the discrete evolution under (39), if it holds initially, rather than just preserved to within an $\mathcal{O}(\Delta t^2)$ truncation error. The discrete equation (33) for evolving $\mathbf{B}$ only contains the equilibrium $\mathbf{\Lambda}^{(0)}$, an antisymmetric tensor, due to the properties of the optimal TRT collision operator. In general one would obtain a discrete evolution equation involving $\mathbf{\Lambda}$, which is not antisymmetric according to (14). Equation (33) is thus a mimetic finite

difference scheme [33, 37, 43] that exactly satisfies a discrete analog of the vector identity $\nabla\cdot(\nabla\times(\mathbf{u}\times\mathbf{B}) \equiv 0$.

6. **Discrete evolution equation for** $\mathrm{Tr}\boldsymbol{\Lambda}$**.** We can also use (29) to construct a discrete evolution equation for the trace of the tensor $\boldsymbol{\Lambda}$,

$$\widetilde{\Lambda}(\mathbf{x}, t+\Delta t) = \omega_{\mathsf{b}}^2 \widetilde{\Lambda}(\mathbf{x}, t-\Delta t) - (1+\omega_{\mathsf{b}}) \sum_{k=0}^{M-1} W_k \boldsymbol{\xi}_k \cdot \mathbf{B}(\mathbf{x}+\boldsymbol{\xi}_k \Delta t, t), \tag{42}$$

where $\widetilde{\Lambda} = \mathrm{Tr}\widetilde{\boldsymbol{\Lambda}} = \sum_k \boldsymbol{\xi}_k \cdot \widetilde{\mathbf{g}}_k$. The contribution from $\boldsymbol{\xi}_k\boldsymbol{\xi}_k : \boldsymbol{\Lambda}^{(0)}$ again vanishes because $\boldsymbol{\Lambda}^{(0)}$ is an antisymmetric tensor. Undoing the transformation (23) by putting $\widetilde{\Lambda} = (1+\Delta t/(2\tau_{\mathsf{o}}))\Lambda$ gives the more time-symmetric evolution equation

$$\frac{\tau_{\mathsf{o}}}{2\Delta t}\left(\left(1+\frac{\Delta t}{2\tau_{\mathsf{o}}}\right)^2 \Lambda(\mathbf{x}, t+\Delta t) - \left(1-\frac{\Delta t}{2\tau_{\mathsf{o}}}\right)^2 \Lambda(\mathbf{x}, t-\Delta t)\right) = -\tau_{\mathsf{o}}\Theta\Delta(\mathbf{x}, t). \tag{43}$$

We can thus evaluate the discrete divergence Δ locally at each grid point from Λ at the same grid point and the adjacent time levels $t \pm \Delta t$. Equation(43) is a second-order accurate approximation to

$$\tau_{\mathsf{o}}\partial_t \Lambda + \Lambda = -\tau_{\mathsf{o}}\Theta\nabla\cdot\mathbf{B}, \tag{44}$$

so $\Lambda = \mathrm{Tr}\boldsymbol{\Lambda}$ plays the role of the extra scalar field in an extended set of Maxwell equations that includes hyperbolic divergence cleaning (see Sec. 7.2). There is no second time derivative $\partial_{tt}\Lambda$ to this order of accuracy because Λ is an odd moment while $\mathbf{B}$ is an even moment. The even relaxation time $\tau_{\mathsf{e}} = \Delta t^2/(4\tau_{\mathsf{o}})$ is $\mathcal{O}(\Delta t^2)$ as $\Delta t \to 0$ with τ_{o} fixed.

7. **First order system and Maxwell's equations.** A more illuminating approach to the telegraph equation (34) for $\mathbf{B}$ is to rewrite it as a first order system in which the magnetic field satisfies the conservation law

$$\partial_t \mathbf{B} + \nabla\cdot\boldsymbol{\Lambda} = 0. \tag{45}$$

This is consistent with (34) provided the flux $\boldsymbol{\Lambda}$ satisfies the evolution equation

$$\boldsymbol{\Lambda} + \tau_{\mathsf{o}}\partial_t\boldsymbol{\Lambda} = -\tau_{\mathsf{o}}\Theta\nabla\mathbf{B} + \boldsymbol{\Lambda}^{(0)}. \tag{46}$$

We can write this in a more familiar form as

$$\partial_t\boldsymbol{\Lambda} + \Theta\nabla\mathbf{B} = -\frac{1}{\tau_{\mathsf{o}}}\left(\boldsymbol{\Lambda} - \boldsymbol{\Lambda}^{(0)}\right). \tag{47}$$

This now matches (14), except $\nabla\cdot\mathbf{M}$ has been replaced with $\nabla\cdot\mathbf{M}^{(0)} = \Theta\nabla\mathbf{B}$ using the properties of the optimal TRT collision operator. We still have a kinetic equation for $\boldsymbol{\Lambda}$, even though (34) is expressed solely in terms of $\mathbf{u}$ and $\mathbf{B}$, because (34) contains two derivatives with respect to time.

7.1. **Evolution of the electric field.** Taking the antisymmetric part of (47) gives

$$\partial_t\mathbf{E} - \Theta\nabla\times\mathbf{B} = -\frac{1}{\tau_{\mathsf{o}}}\left(\mathbf{E} + \mathbf{u}\times\mathbf{B}\right), \tag{48}$$

where the electric field $\mathbf{E}$ has components $E_\gamma = -\frac{1}{2}\epsilon_{\alpha\beta\gamma}\Lambda_{\alpha\beta}$ and $\mathbf{E}^{(0)} = -\mathbf{u}\times\mathbf{B}$. This exactly matches the evolution equation [8]

$$\partial_t\mathbf{E} - c^2\nabla\times\mathbf{B} = -\frac{1}{\tau_{\mathsf{c}}}\left(\mathbf{E} + \mathbf{u}\times\mathbf{B}\right) \tag{49}$$

obtained by combining Maxwell's equation

$$\nabla\times\mathbf{B} = \mu_0\mathbf{J} + \frac{1}{c^2}\partial_t\mathbf{E} \tag{50}$$

with Ohm's law

$$\mathbf{J} = \sigma(\mathbf{E} + \mathbf{u}\times\mathbf{B}). \tag{51}$$

These equations are written in SI units with permeability of free space μ_0, speed of light c, and conductivity σ. The divergence of (49) gives the evolution equation [8]

$$\tau_\mathsf{c}\partial_t\varrho + \varrho = -\epsilon_0\nabla\cdot(\mathbf{u}\times\mathbf{B}) \tag{52}$$

for the electric charge density $\varrho = \epsilon_0\nabla\cdot\mathbf{E}$, where $\epsilon_0 = 1/(\mu_0 c^2)$ is the permittivity of free space, and $\tau_\mathsf{c} = \epsilon_0/\sigma$ is the charge relaxation time. The charge density decays as $\exp(-t/\tau_\mathsf{c})$ if the right-hand side vanishes. The resistivity is $\eta = c^2\tau_\mathsf{c}$ in these units, giving $\mathbf{J} = \eta(\nabla\times\mathbf{B} - c^{-2}\partial_t\mathbf{E})$. The last term can be neglected for non-relativistic flows with velocity $|\mathbf{u}| \ll c$, leaving $\mathbf{J} = \eta\nabla\times\mathbf{B}$ as in Sec. 2.

We can thus derive the resistive MHD induction equation from our lattice Boltzmann formulation using solely the "non-relativistic" approximation $|\mathbf{u}| \ll \Theta^{1/2}$, where $\Theta^{1/2}$ is the lattice speed of light, to neglect $\tau_\mathsf{o}\partial_t\Lambda$ in (46) and $\partial_t\mathbf{E}$ in (48). We do not need the Chapman–Enskog expansion used in Sec. 2.2, because the effect of the optimal TRT collision operator has been to replace $\mathbf{M}$ with $\mathbf{M}^{(0)}$ in the discrete evolution equation for $\mathbf{B}$. The formula $\eta = \tau_\mathsf{o}\Theta$ relating the resistivity to the relaxation time and the lattice speed of light is equivalent to $\eta = \tau_\mathsf{c}c^2$ in SI units.

7.2. **Extended Maxwell equations with divergence cleaning.** Taking the divergence of (34) and omitting the $\mathcal{O}(\Delta t^2)$ truncation error gives

$$\tau_\mathsf{o}\partial_{tt}(\nabla\cdot\mathbf{B}) + \partial_t(\nabla\cdot\mathbf{B}) = \tau_\mathsf{o}\Theta\nabla^2(\nabla\cdot\mathbf{B}). \tag{53}$$

The contribution from the double divergence $\nabla\nabla : \mathbf{\Lambda}^{(0)}$ vanishes because $\mathbf{\Lambda}^{(0)}$ is an antisymmetric tensor, so we obtain this closed telegraph equation for $\nabla\cdot\mathbf{B}$.

The Faraday–Maxwell equation implies that $\partial_t(\nabla\cdot\mathbf{B}) = 0$ as $\nabla\cdot(\nabla\times\mathbf{E}) \equiv 0$. However, we can obtain (53) from an extension of Maxwell's equations that implements what is known as hyperbolic divergence cleaning [2, 9, 15, 43]. The magnetic field is postulated to evolve according to

$$\partial_t\mathbf{B} + \nabla\times\mathbf{E} + \nabla\Lambda = 0, \tag{54}$$

with an extra scalar field Λ that is postulated to evolve according to

$$\tau_\mathsf{o}\partial_t\Lambda + \Lambda = -\tau_\mathsf{o}\Theta\nabla\cdot\mathbf{B}. \tag{55}$$

The latter coincides with (44) above. This extension of Maxwell's equations is designed to diffuse away any nonzero $\nabla\cdot\mathbf{B}$ created by numerical errors, while keeping the maximum signal propagation speed finite so that explicit time integration schemes remain stable. It can be interpreted as a continuous-in-time formulation of the Boris projection method that projects $\mathbf{B}$ onto the space of divergence-free vector fields at every discrete timestep [4, 5]. We can also interpret (54) as a Helmholtz decomposition of $\partial_t\mathbf{B}$ into a divergence-free part $\nabla\times\mathbf{E}$ and a curl-free part $\nabla\Lambda$. We have established that the $\nabla\times\mathbf{E}$ part reproduces the combination of the Faraday–Maxwell equation and Ohm's law, and the $\nabla\Lambda$ part reproduces the hyperbolic divergence cleaning equations.

The optimal TRT collision operator offers a particularly straightforward lattice Boltzmann formulation for the hyperbolic divergence cleaning equations. Baty *et*

al. [2] introduced Λ as an additional scalar field represented by additional distribution functions. Dellar [15] later transformed (10) with a general tensor $\mathbf{\Lambda}$ into (54) using a gauge transformation to absorb a contribution from the first-order Chapman–Enskog approximation to the symmetric and traceless part of $\mathbf{\Lambda}$. This transformation is not required in the optimal TRT formulation. The evolution equation (47) for $\mathbf{\Lambda}$ only involves the equilibrium $\nabla\cdot\mathbf{M}^{(0)} = \Theta\nabla\mathbf{B}$, while the evolution of $\mathbf{\Lambda}$ through (14) or its equivalent for a general collision operator involves the divergence of the evolving tensor $\mathbf{M}$.

The evolution of $\nabla\cdot\mathbf{B}$ under (54) and (55) reduces to the parabolic divergence cleaning equation (18) when $\mathbf{B}$ evolves on timescales much longer than τ_o. In this approximation we recover [11]

$$\operatorname{Tr}\mathbf{\Lambda} \approx -\tau_\mathsf{o}\Theta\nabla\cdot\mathbf{B}, \tag{56}$$

so $\operatorname{Tr}\mathbf{\Lambda}$ being small is a consistent proxy for $\nabla\cdot\mathbf{B}$ being small. This approximation is made precise by the exact relation (43) between Δ and Λ in the discrete system.

8. **Initialisation.** Like any scheme using three time levels, the macroscopic finite difference scheme derived from the optimal TRT lattice Boltzmann equation needs two sets of initial conditions at times $t = 0$ and $t = \Delta t$ to determine the solution at $t = 2\Delta t$. The lattice Boltzmann equation itself only needs the first set at $t = 0$. The natural approach is to use one step of the lattice Boltzmann equation to advance from $t = 0$ to $t = \Delta t$.

In principle, the initial conditions for a lattice Boltzmann equation should initialise the non-equilibrium parts of the distribution functions consistently with the structure of slowly varying solutions. For example, the initial $\mathbf{\Lambda}$ should be consistent with $\mathbf{\Lambda} = \mathbf{\Lambda}^{(0)} - \tau_\mathsf{o}\Theta\nabla\mathbf{B} + \cdots$ according to the Chapman–Enskog expansion in Sec. 2.2 that leads to the resistive MHD induction equation. However, many lattice Boltzmann simulations simply initialise the distribution functions to their equilibrium values, thus neglecting non-ideal effects like resistivity or viscosity. The non-equilibrium distributions are expected to adjust during a short initial transient to become consistent with the Chapman–Enskog expansion that describes slowly varying solutions.

Given initial conditions $\mathbf{g}_k = \mathbf{g}_k^{(0)}$ at $t = 0$ we can take one step with the lattice Boltzmann equation to determine

$$\mathbf{g}_k(\mathbf{x}, \Delta t) = \mathbf{g}_k^{(0)}(\mathbf{x} - \boldsymbol{\xi}_k\Delta t, 0). \tag{57}$$

This holds for all choices of collision operator because the initial conditions at $t = 0$ are in equilibrium. Taking the zeroth moment of (57) gives the second set of initial conditions:

$$\begin{aligned}
\mathbf{B}(\mathbf{x}, \Delta t) &= \sum_{k=0}^{M-1} \mathbf{g}_k^{(0)}(\mathbf{x} - \boldsymbol{\xi}_k\Delta t, 0), \\
&= \sum_{k=0}^{M-1} W_k\mathbf{B}(\mathbf{x} - \boldsymbol{\xi}_k\Delta t, 0) + \frac{1}{\Theta}\sum_{k=0}^{M-1} W_k\boldsymbol{\xi}_k\cdot\mathbf{\Lambda}^{(0)}(\mathbf{x} - \boldsymbol{\xi}_k\Delta t, 0), \\
&= \mathbf{B} + \tfrac{1}{2}\Theta\Delta t^2\nabla^2\mathbf{B} + \Delta t\nabla\times(\mathbf{u}\times\mathbf{B}) + \mathcal{O}(\Delta t^3).
\end{aligned} \tag{58}$$

All the fields and their spatial derivatives in the last line are evaluated at $t = 0$. Equation (58) is equivalent to the previous discrete evolution equation (32) with ω_b set to zero to eliminate the contribution from $\mathbf{B}(\mathbf{x}, -\Delta t)$. Setting $\omega_\mathsf{b} = 0$ is

equivalent to setting $\tau_{\mathsf{o}} = \Delta t/2$, which gives the coefficient $\tau_{\mathsf{o}}\Theta\Delta t = \Theta\Delta t^2/2$ for $\nabla^2\mathbf{B}$ in (58). Equation (58) is equivalent to taking the first timestep using Junk & Rao's scheme [35], which in turn is equivalent to the simplest form of Inamuro's lattice kinetic scheme with no finite-difference correction of the diffusion [34].

The initial magnetic field should satisfy the discrete divergence-free condition $\Delta = 0$. We can construct such a field by expressing $\mathbf{B} = \nabla\times\mathbf{A}$ as the curl of a vector potential $\mathbf{A}$, then discretising this relation using

$$\mathbf{B}(\mathbf{x},0) = \frac{1}{\Theta\Delta t}\sum_{k=0}^{M-1} W_k\boldsymbol{\xi}_k\times\mathbf{A}(\mathbf{x}+\boldsymbol{\xi}_k\Delta t,0). \tag{59}$$

The discrete divergence of this expression vanishes,

$$\sum_{j=0}^{M-1} W_j\boldsymbol{\xi}_j\cdot\mathbf{B}(\mathbf{x}+\boldsymbol{\xi}_j\Delta t,0) = \frac{1}{\Theta\Delta t}\sum_{j=0}^{M-1}\sum_{k=0}^{M-1} W_jW_k(\boldsymbol{\xi}_j\times\boldsymbol{\xi}_k)\cdot\mathbf{A}\big(\mathbf{x}+(\boldsymbol{\xi}_j+\boldsymbol{\xi}_k)\Delta t,0\big) = 0, \tag{60}$$

because the summand is antisymmetric in j and k. The discrete divergence and curl operators thus exactly satisfy a discrete form of the vector identity $\nabla\cdot(\nabla\times\mathbf{A}) \equiv 0$ for all vector fields $\mathbf{A}$. This is another example of the mimetic properties satisfied by the lattice-adapted finite difference operators [33, 37, 43].

9. **Discrete macroscopic equations for hydrodynamics.** Applying the same approach to the hydrodynamic lattice Boltzmann scheme in Sec. 2.1 with the optimal TRT collision operator gives discrete equations for evolving the fluid density and velocity across three time levels:

$$\begin{aligned}
&\rho(\mathbf{x},t+\Delta t)\\
&= -\hat{\omega}_{\mathsf{b}}\rho(\mathbf{x},t-\Delta t) + (1-\hat{\omega}_{\mathsf{b}})\frac{1}{\theta}\sum_{k=0}^{N-1} w_k\boldsymbol{\xi}_k\cdot(\rho\mathbf{u})(\mathbf{x}-\boldsymbol{\xi}_k\Delta t,t)\\
&\quad + (1+\hat{\omega}_{\mathsf{b}})\left\{\sum_{k=0}^{N-1} w_k\rho(\mathbf{x}-\boldsymbol{\xi}_k\Delta t,t) + \frac{1}{2\theta^2}\sum_{k=0}^{N-1} w_k(\boldsymbol{\xi}_k\boldsymbol{\xi}_k-\theta\mathsf{I}):\widehat{\boldsymbol{\Pi}}^{(0)}(\mathbf{x}-\boldsymbol{\xi}_k\Delta t,t)\right\},
\end{aligned} \tag{61}$$

where $(\rho\mathbf{u})(\mathbf{x}-\boldsymbol{\xi}_k\Delta t,t)$ denotes the product $\rho(\mathbf{x}-\boldsymbol{\xi}_k\Delta t,t)\mathbf{u}(\mathbf{x}-\boldsymbol{\xi}_k\Delta t,t)$, the pressureless part of the equilibrium momentum flux is $\widehat{\boldsymbol{\Pi}}^{(0)} = \boldsymbol{\Pi}^{(0)} - \rho\theta\mathsf{I}$, and

$$\begin{aligned}
&(\rho\mathbf{u})(\mathbf{x},t+\Delta t)\\
&= \hat{\omega}_{\mathsf{b}}(\rho\mathbf{u})(\mathbf{x},t-\Delta t) + (1-\hat{\omega}_{\mathsf{b}})\frac{1}{\theta}\sum_{k=0}^{N-1} w_k\boldsymbol{\xi}_k\boldsymbol{\xi}_k\cdot(\rho\mathbf{u})(\mathbf{x}-\boldsymbol{\xi}_k\Delta t,t)\\
&\quad + (1+\hat{\omega}_{\mathsf{b}})\left\{\sum_{k=0}^{N-1} w_k\boldsymbol{\xi}_k\rho(\mathbf{x}-\boldsymbol{\xi}_k\Delta t) + \frac{1}{2\theta^2}\sum_{k=0}^{N-1} w_k\boldsymbol{\xi}_k(\boldsymbol{\xi}_k\boldsymbol{\xi}_k-\theta\mathsf{I}):\widehat{\boldsymbol{\Pi}}^{(0)}(\mathbf{x}-\boldsymbol{\xi}_k\Delta t,t)\right\}.
\end{aligned} \tag{62}$$

The hydrodynamic relaxation rate $\hat{\omega}_{\mathsf{b}}$ that controls the viscosity can be chosen independently from the magnetic relaxation rate ω_{b} that controls the resistivity. The differing signs of the $\hat{\omega}_{\mathsf{b}}$ terms in (61) and (62) arise because $\rho = \sum_k f_k$ is an even moment of the f_k, while $\rho\mathbf{u} = \sum_k \boldsymbol{\xi}_k f_k$ is an odd moment. As before, we can construct a second set of initial conditions for this three-time-level finite difference scheme by taking a first step with $\hat{\omega}_{\mathsf{b}} = 0$ to remove the dependence on the prior time level $t = -\Delta t$. The properties of this system will be described elsewhere. It is included here only as a necessary part of constructing a complete macroscopic finite difference scheme for magnetohydrodynamics.

10. **Numerical experiments.** We consider a simulation of the two-dimensional doubly-periodic coalescence instability [11, 38, 39] starting from the initial conditions with uniform density $\rho_0 = 1$ and

$$\begin{aligned} B_x &= \pi \sin(2\pi y), & u_x &= \frac{1}{5} y \exp(-10(x^2+y^2)), \\ B_y &= \pi \sin(2\pi x), & u_y &= -\frac{1}{5} x \exp(-10(x^2+y^2)), \end{aligned} \tag{63}$$

in the domain $[-1,1]^2$. The initial magnetic field corresponds to $\mathbf{B} = \nabla\times(A_z\mathbf{e}_z)$ with $A_z = (\cos(2\pi x)-\cos(2\pi y))/2$ and $\mathbf{e}_z$ a unit vector in the z direction. This field represents a symmetrical array of magnetic islands, an equilibrium configuration, that is destabilised by the fluid flow. The islands merge in pairs by forming intense current sheets with large current densities. The initial velocity field is larger than some used previously to reduce the time spent in the linear regime before the solution starts to evolve nonlinearly. Figure 2 shows the current $J_z = \mathbf{e}_z \cdot \nabla\times\mathbf{B}$ for the initial conditions at $t = 0$, and at the later times $t = 1.0$, $t = 1.5$ and $t = 2.0$. The simulations used a grid of 1024×1024 points, diffusion coefficients $\eta = \nu = 0.01$, and a nominal Mach number 0.044.

Figure 3 shows the discrete ℓ^2 norms of the differences between the density, velocity, and magnetic fields computed using the macroscopic finite difference scheme for ρ, $\mathbf{u}$ and $\mathbf{B}$ across three time levels, and using the optimal TRT lattice Boltzmann scheme with a D2Q9 lattice for the $\tilde{f}_k$ and two copies of the D2Q5 lattice for the $\widetilde{\mathbf{g}}_k$. The differences between the two solutions can all be attributed to floating point round-off errors. The computations were run using 128-bit IEEE binary floating point arithmetic with a precision of roughly 33 decimal digits. The hydrodynamic part of the lattice Boltzmann scheme was formulated using the variables $\delta f_k = f_k - w_k$ and $\delta f_k^{(0)} = f_k^{(0)} - w_k$ following Skordos [48]. The macroscopic finite difference scheme was formulated using the density perturbation $\delta\rho = \rho - \rho_0$. These two changes alleviate the effects of round-off errors when forming $f_k - f_k^{(0)}$ in the collision operator, and when applying finite difference operators to values of ρ at adjacent grid points. Figure 3 also shows the discrete ℓ^2 norm of the discrete divergence Δ. This starts around 10^{-31} and decreases with time due to the diffusive behaviour of the telegraph equation (53) on timescales longer than τ_o.

11. **Conclusion.** The lattice Boltzmann approach embeds the target system of partial differential equations into a larger linear, constant coefficient hyperbolic system. All nonlinearity is confined to algebraic source terms that model collisions between particles. The hyperbolic part may be readily discretised by integration along its characteristics, and combined with local solution of the algebraic part at individual grid points [13, 30].

The two-relaxation-time (TRT) collision operator combines the discrete velocities into anti-parallel pairs, called links or dumbbells, and assigns odd and even relaxation times τ_o and τ_e to the odd and even combinations of the distribution functions [16, 20, 21, 22, 24, 25, 26, 27]. The particular "magic" combination with $\tau_\mathsf{e}\tau_\mathsf{o} = (3/16)\Delta t^2$ places the point of zero tangential velocity precisely half-way between grid points in simulations of axis-aligned Poiseuille flow with bounce-back boundary conditions [23, 24, 27]. A different combination with $\tau_\mathsf{e}\tau_\mathsf{o} = (1/4)\Delta t^2$ has been named the "optimal TRT" because it greatly simplifies both the structure of the recurrence relations governing steady solutions of lattice Boltzmann equations, and the characteristic polynomials governing the stability of plane wave solutions

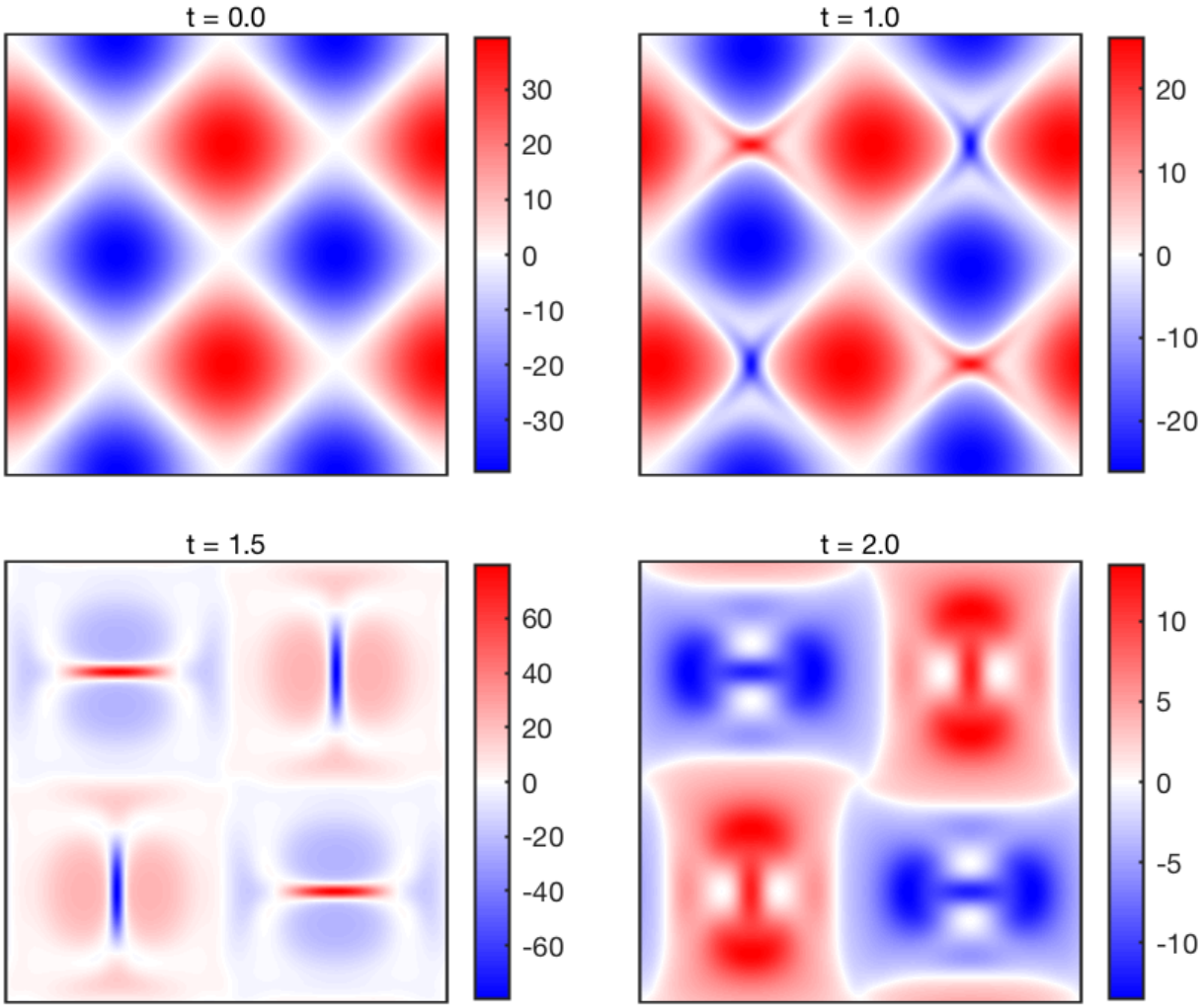

FIGURE 2. The current $J_z = \mathbf{e}_z \cdot \nabla \times \mathbf{B}$ at the four times $t = 0.0$, 1.0, 1.5 and 2.0. The magnetic islands in the initial regular array merge in pairs by forming the current sheets visible at $t = 1.5$.

[16, 21, 25, 26]. Ginzburg [21, 22] derived a macroscopic finite difference scheme for the mass density from an optimal TRT lattice Boltzmann formulation of an advection-diffusion equation.

We have re-interpreted the optimal combination $\tau_e \tau_o = (1/4)\Delta t^2$ as setting the dimensionless forward relaxation rate ω_f to unity, hence setting the forward-propagating distribution functions to equilibrium at every timestep. This allowed us to derive closed evolution equations for every moment of the distribution functions across three time levels, involving only the macroscopic variables at adjacent grid points. This gives a more intuitive derivation of the earlier result by Ginzburg [21, 22]. Moreover, the equivalent equations for the macroscopic variables are more easily interpreted as a first-order system: the expected conservation law and a first-order kinetic equation for the flux. In particular, we derived a closed finite difference scheme for evolving the magnetic field across three time levels. The resulting macroscopic finite difference scheme for the MHD equations reduces the required number of degrees of freedom per grid point from $9 + 2 \times 5 = 19$ to $2 \times (1 + 2 + 2) = 10$ in two dimensions. We can replace all the distribution functions f_k and $\mathbf{g}_k$ at one time level with just the fluid density, velocity and magnetic field at two consecutive time levels.

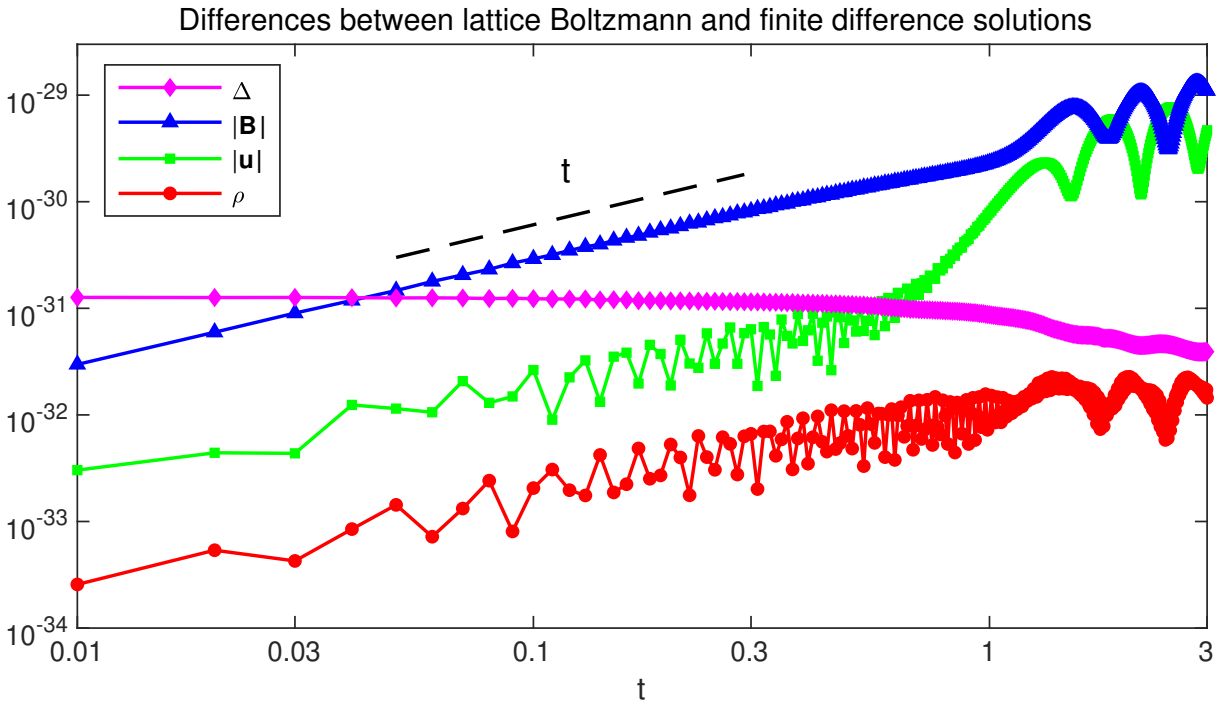

FIGURE 3. Discrete ℓ^2 norms of the differences between the density, velocity, and magnetic fields computed using the optimal TRT lattice Boltzmann equation and the macroscopic finite difference scheme, both using 128-bit arithmetic. These differences initially increase linearly with time (dashed line $- - -$). The ℓ^2 norm of the discrete divergence Δ decreases over time due to the diffusive properties of the divergence cleaning equations on timescales much longer than τ_o.

In this formulation, the resistive MHD induction equation follows solely from a non-relativistic assumption without requiring the usual Chapman–Enskog expansion. We also obtain an additional scalar contribution linked to $\nabla\cdot\mathbf{B}$ in the evolution equation for $\mathbf{B}$, so our scheme implements the hyperbolic divergence cleaning equations [2, 9, 15, 43]. The closed finite difference scheme for the magnetic field defines a natural discrete divergence operator acting on the electric field tensor $\mathbf{\Lambda}$. Applying the same operator to the magnetic field gives a natural discrete approximation to $\nabla\cdot\mathbf{B}$ that satisfies a closed discrete telegraph equation. This discrete approximation to $\nabla\cdot\mathbf{B} = 0$ is maintained at the level of floating point round-off error when $\mathbf{B}$ is consistently initialised using a discrete approximation to $\mathbf{B} = \nabla\times\mathbf{A}$. We have thus constructed a mimetic finite difference [33, 37, 43] scheme, or equivalently a constrained transport scheme [18, 52], for magnetohydrodynamics. This scheme exactly preserves a discrete analog of $\nabla\cdot\mathbf{B} = 0$ because it satisfies an exact discrete analog of $\nabla\cdot(\nabla\times\mathbf{E}) \equiv 0$.

Acknowledgments. The author thanks Dr Thomas Bellotti for pointing him to ref. [21]. The computations were performed using the Advanced Research Computing facilities of the University of Oxford [44].

Appendix. Discrete Laplacian and divergence operators. The early development of lattice gas and lattice Boltzmann algorithms for multiphase flows introduced lattice-adapted finite difference formulae using the discrete velocities $\boldsymbol{\xi}_k$

and weights W_k to approximate the momentum gradient [45], the colour gradient [29, 46], the pseudopotential gradient [47], and the Laplacian [6]. A compilation of these formulae may be found in [51].

For any smooth scalar function f, we can expand $f(\mathbf{x}+\boldsymbol{\xi}_k\Delta t)$ in a Taylor series around $\mathbf{x}$ for small Δt and evaluate

$$\begin{aligned}\sum_{k=0}^{M-1} W_k f(\mathbf{x}+\boldsymbol{\xi}_k\Delta t) &= \sum_{k=0}^{M-1} W_k \bigg(f(\mathbf{x}) + \Delta t \xi_{k\alpha}\frac{\partial f}{\partial x_\alpha} + \frac{1}{2}\Delta t^2 \xi_{k\alpha}\xi_{k\beta}\frac{\partial^2 f}{\partial x_\alpha \partial x_\beta} \\ &\quad + \frac{1}{6}\Delta t^3 \xi_{k\alpha}\xi_{k\beta}\xi_{k\gamma}\frac{\partial^3 f}{\partial x_\alpha \partial x_\beta \partial x_\gamma} + \mathcal{O}(\Delta t^4)\bigg), \qquad (64)\\ &= f(\mathbf{x}) + \frac{1}{2}\Delta t^2 \Theta \nabla^2 f + \mathcal{O}(\Delta t^4),\end{aligned}$$

using the normalisation, symmetry, and isotropy properties of the weights and discrete velocities:

$$\sum_{k=0}^{M-1} W_k = 1, \quad \sum_{k=0}^{M-1} W_k \boldsymbol{\xi}_k = 0, \quad \sum_{k=0}^{M-1} W_k \boldsymbol{\xi}_k \boldsymbol{\xi}_k = \Theta \mathsf{I}, \quad \sum_{k=0}^{M-1} W_k \boldsymbol{\xi}_k \boldsymbol{\xi}_k \boldsymbol{\xi}_k = 0. \qquad (65)$$

Similarly, for any smooth vector function $\mathbf{F}$ we can evaluate

$$\begin{aligned}\sum_{k=0}^{M-1} W_k \boldsymbol{\xi}_k \cdot \mathbf{F}(\mathbf{x}+\boldsymbol{\xi}_k\Delta t) &= \sum_{k=0}^{M-1} W_k \xi_{k\alpha} \bigg(F_\alpha(\mathbf{x}) + \Delta t \xi_{k\beta}\frac{\partial F_\alpha}{\partial x_\beta} + \frac{1}{2}\Delta t^2 \xi_{k\beta}\xi_{k\gamma}\frac{\partial^2 F_\alpha}{\partial x_\beta \partial x_\gamma} \\ &\quad + \frac{1}{6}\Delta t^3 \xi_{k\beta}\xi_{k\gamma}\xi_{k\delta}\frac{\partial^3 F_\alpha}{\partial x_\beta \partial x_\gamma \partial x_\delta} + \mathcal{O}(\Delta t^4)\bigg), \qquad (66)\\ &= \Delta t \Theta \nabla \cdot \mathbf{F} + \mathcal{O}(\Delta t^3).\end{aligned}$$

We thus have the second-order accurate finite differerence approximations [51]

$$\frac{1}{\Theta \Delta t}\sum_{k=0}^{M-1} W_k \boldsymbol{\xi}_k \cdot \mathbf{F}(\mathbf{x}+\boldsymbol{\xi}_k\Delta t) = \nabla \cdot \mathbf{F} + \mathcal{O}(\Delta t^2), \qquad (67a)$$

$$\frac{2}{\Theta \Delta t^2}\left(\sum_{k=0}^{M-1} W_k f(\mathbf{x}+\boldsymbol{\xi}_k\Delta t) - f(\mathbf{x})\right) = \nabla^2 f + \mathcal{O}(\Delta t^2), \qquad (67b)$$

where $f(\mathbf{x})$ is outside the sum. These reduce to the standard centred finite difference formulae on the D2Q5 and D3Q7 lattices for all symmetric choices of weights W_k that satisfy (65).

REFERENCES

[1] M. G. Ancona, Fully Lagrangian and lattice Boltzmann methods for solving systems of conservation equations, *J. Comput. Phys.*, **115** (1994), 107–120.

[2] H. Baty, F. Drui, P. Helluy, E. Franck, C. Klingenberg and L. Thanhäuser, A robust and efficient solver based on kinetic schemes for magnetohydrodynamics (MHD) equations, *Appl. Math. Comput.*, **440** (2023), 127667, 18 pages.

[3] T. Bellotti, B. Graille and M. Massot, Finite difference formulation of any lattice Boltzmann scheme, *Numer. Math.*, **152** (2022), 1–40.

[4] J. P. Boris, Relativistic plasma simulation – optimization of a hybrid code, in *Proceedings of the 4th Conference on Numerical Simulation of Plasmas* (eds. J. P. Boris and R. A. Shanny), Naval Research Laboratory, Washington, DC, 1972, 3–67.

[5] J. U. Brackbill and D. C. Barnes, The effect of nonzero $\nabla \cdot \mathbf{B}$ on the numerical solution of the magnetohydrodynamic equations, *J. Comput. Phys.*, **35** (1980), 426–430.

[6] H. Chen, S. Chen, G. Doolen and Y. C. Lee, Simple lattice gas models for waves, *Complex Syst.*, **2** (1988), 259–267.
[7] S. Chen and G. D. Doolen, Lattice Boltzmann method for fluid flows, *Annu. Rev. Fluid Mech.*, **30** (1998), 329–364.
[8] P. A. Davidson, *An Introduction to Electrodynamics*, Oxford University Press, Oxford, 2019.
[9] A. Dedner, F. Kemm, D. Kröner, C. D. Munz, T. Schnitzer and M. Wesenberg, Hyperbolic divergence cleaning for the MHD equations, *J. Comput. Phys.*, **175** (2002), 645–673.
[10] S. Dellacherie, Construction and analysis of lattice Boltzmann methods applied to a 1D convection-diffusion equation, *Acta Applic. Math.*, **131** (2014), 69–140.
[11] P. J. Dellar, Lattice kinetic schemes for magnetohydrodynamics, *J. Comput. Phys.*, **179** (2002), 95–126.
[12] P. J. Dellar, Incompressible limits of lattice Boltzmann equations using multiple relaxation times, *J. Comput. Phys.*, **190** (2003), 351–370.
[13] P. J. Dellar, An interpretation and derivation of the lattice Boltzmann method using Strang splitting, *Comput. Math. Applic.*, **65** (2013), 129–141.
[14] P. J. Dellar, Relativistic properties and invariants of the Du Fort–Frankel scheme for the one-dimensional Schrödinger equation, *J. Comput. Phys. X*, **2** (2019), 100004, 18 pages.
[15] P. J. Dellar, Hyperbolic divergence cleaning in lattice Boltzmann magnetohydrodynamics, *Commun. Comput. Phys.*, **33** (2023), 245–272.
[16] D. d'Humières and I. Ginzburg, Viscosity independent numerical errors for Lattice Boltzmann models: From recurrence equations to "magic" collision numbers, *Comput. Math. Applic.*, **58** (2009), 823–840.
[17] E. C. Du Fort and S. P. Frankel, Stability conditions in the numerical treatment of parabolic differential equations, *Math. Tables Other Aids Comput.*, **7** (1953), 135–152.
[18] C. R. Evans and J. F. Hawley, Simulation of magnetohydrodynamic flows – A constrained transport method, *Astrophys. J.*, **332** (1988), 659–677.
[19] R. Fučík and R. Straka, Equivalent finite difference and partial differential equations for the lattice Boltzmann method, *Comput. Math. Applic.*, **90** (2021), 96–103.
[20] I. Ginzburg, Equilibrium-type and link-type lattice Boltzmann models for generic advection and anisotropic-dispersion equation, *Adv. Water Res.*, **28** (2005), 1171–1195.
[21] I. Ginzburg, *Une Variation sur les Propriétés Magiques de modèles de Boltzmann pour L'écoulement Microscopique et Macroscopique*, Thèse d'habilitation, Université Pierre et Marie Curie, Paris, 2009, available from `https://hal.inrae.fr/tel-02591565`.
[22] I. Ginzburg, Truncation errors, exact and heuristic stability analysis of two-relaxation-times lattice Boltzmann schemes for anisotropic advection-diffusion equation, *Commun. Comp. Phys.*, **11** (2012), 1439–1502.
[23] I. Ginzbourg and M. P. Adler, Boundary flow condition analysis for the three-dimensional lattice Boltzmann model, *J. Phys. II France*, **4** (1994), 191–214.
[24] I. Ginzburg and D. d'Humières, Multireflection boundary conditions for lattice Boltzmann models, *Phys. Rev. E*, **68** (2003), 066614, 30 pages.
[25] I. Ginzburg and D. d'Humières, Lattice Boltzmann and analytical modeling of flow processes in anisotropic and heterogeneous stratified aquifers, *Adv. Water Resour.*, **30** (2007), 2202–2234.
[26] I. Ginzburg, D. d'Humières and A. Kuzmin, Optimal stability of advection-diffusion lattice Boltzmann models with two relaxation times for positive/negative equilibrium, *J. Stat. Phys.*, **139** (2010), 1090–1143.
[27] I. Ginzburg, F. Verhaeghe and D. d'Humières, Two-relaxation-time Lattice Boltzmann scheme: About parametrization, velocity, pressure and mixed boundary conditions, *Commun. Comput. Phys.*, **3** (2008), 427–478.
[28] D. Gottlieb and B. Gustafsson, Generalized Du Fort–Frankel methods for parabolic initial-boundary value problems, *SIAM J. Numer. Anal.*, **13** (1976), 129–144.
[29] A. K. Gunstensen, D. H. Rothman, S. Zaleski and G. Zanetti, Lattice Boltzmann model of immiscible fluids, *Phys. Rev. A*, **43** (1991), 4320–4327.
[30] X. He, S. Chen and G. D. Doolen, A novel thermal model of the lattice Boltzmann method in incompressible limit, *J. Comput. Phys.*, **146** (1998), 282–300.
[31] M. Hénon, Viscosity of a lattice gas, *Complex Syst.*, **1** (1987), 763–789.
[32] S. Hou, Q. Zou, S. Chen, G. Doolen and A. C. Cogley, Simulation of cavity flow by the lattice Boltzmann method, *J. Comput. Phys.*, **118** (1995), 329–347.

[33] J. M. Hyman and M. Shashkov, Mimetic discretizations for Maxwell's equations, *J. Comput. Phys.*, **151** (1999), 881–909.
[34] T. Inamuro, A lattice kinetic scheme for incompressible viscous flows with heat transfer, *Phil. Trans. Roy. Soc. Lond. Ser. A*, **360** (2002), 477–484.
[35] M. Junk and S. V. R. Rao, A new discrete velocity method for Navier–Stokes equations, *J. Comput. Phys.*, **155** (1999), 178–198.
[36] P. Lallemand, L.-S. Luo, M. Krafczyk and W.-A. Yong, The lattice Boltzmann method for nearly incompressible flows, *J. Comput. Phys.*, **431** (2021), 109713, 52 pages.
[37] K. Lipnikov, G. Manzini and M. Shashkov, Mimetic finite difference method, *J. Comput. Phys.*, **257** (2014), 1163–1227.
[38] D. W. Longcope and H. R. Strauss, The coalescence instability and the development of current sheets in two-dimensional magnetohydrodynamics, *Phys. Fluids B*, **5** (1993), 2858–2869.
[39] C. Marliani and H. R. Strauss, Reconnection of coalescing magnetic islands, *Phys. Plasmas*, **6** (1999), 495–502.
[40] D. O. Martínez, S. Chen and W. H. Matthaeus, Lattice Boltzmann magnetohydrodynamics, *Phys. Plasmas*, **1** (1994), 1850–1867.
[41] Y. H. Qian, D. d'Humières and P. Lallemand, Lattice BGK models for the Navier–Stokes equation, *Europhys. Lett.*, **17** (1992), 479–484.
[42] Y. H. Qian and S. A. Orszag, Lattice BGK models for the Navier–Stokes equation: Nonlinear deviation in compressible regimes, *Europhys. Lett.*, **21** (1993), 255–259.
[43] J. D. Ramshaw, A method for enforcing the solenoidal condition on magnetic field in numerical calculations, *J. Comput. Phys.*, **52** (1983), 592–596.
[44] A. Richards, *University of Oxford Advanced Research Computing*, Technical Note, 2015, available from doi:10.5281/zenodo.22558.
[45] D. H. Rothman, Negative viscosity lattice gases, *J. Stat. Phys.*, **56** (1989), 517–524.
[46] D. H. Rothman and S. Zaleski, *Lattice-Gas Cellular Automata*, Cambridge University Press, Cambridge, 1997.
[47] X. Shan and H. Chen, Lattice Boltzmann model for simulating flows with multiple phases and components, *Phys. Rev. E*, **47** (1993), 1815–1819.
[48] P. A. Skordos, Initial and boundary conditions for the lattice Boltzmann method, *Phys. Rev. E*, **48** (1993), 4823–4842.
[49] G. Strang, On the construction and comparison of difference schemes, *SIAM J. Numer. Anal.*, **5** (1968), 506–517.
[50] B. K. Swartz, The construction and comparison of finite difference analogs of some finite element schemes, in *Mathematical Aspects of Finite Elements in Partial Differential Equations* (ed. C. de Boor), Academic Press, 1974, 279–312.
[51] S. P. Thampi, S. Ansumali, R. Adhikari and S. Succi, Isotropic discrete Laplacian operators from lattice hydrodynamics, *J. Comput. Phys.*, **234** (2013), 1–7.
[52] G. Tóth, The $\nabla \cdot \mathbf{B} = 0$ constraint in shock-capturing magnetohydrodynamics codes, *J. Comput. Phys.*, **161** (2000), 605–652.

Received December 2022; revised August 2023; early access September 2023.